

Contributions of the troposphere and stratosphere to CH₄ model biases

Zhiting Wang¹, Thorsten Warneke¹, Nicholas M. Deutscher^{1,2}, Justus Notholt¹, Ute Karstens³, Marielle Saunois⁴, Matthias Schneider⁵, Ralf Sussmann⁶, Harjinder Sembhi⁷, David W. T. Griffith², Dave F. Pollard⁸, Rigel Kivi⁹, Christof Petri¹, Voltaire A. Velazco², Michel Ramonet¹⁰, Huilin Chen^{11,12}

(1) Institute of Environmental Physics, University of Bremen, Germany

(2) Centre for Atmospheric Chemistry, School of Chemistry, University of Wollongong, Wollongong, New South Wales, Australia

10 (3) Max Planck Institute for Biogeochemistry, Germany

(4) Laboratoire des Sciences du Climat et de l'Environnement, France

(5) Karlsruhe Institute of Technology, IMK-ASF, Karlsruhe, Germany

(6) Karlsruhe Institute of Technology, IMK-IFU, Garmisch-Partenkirchen, Germany

15 (7) Earth Observation Science, Department of physics and Astronomy, University of Leicester, Leicester, UK

(8) National Institute of Water and Atmospheric Research (NIWA), Wellington, New Zealand

(9) Finnish Meteorological Institute Arctic Research Center, FMI-ARC, Finland

(10) Laboratoire des Sciences du Climat et de l'Environnement, LSCE/IPSL, CEA-CNRS-UVSQ, Université Paris Saclay, 91191, Gif-Sur-Yvette, France

20 (11) Center for Isotope Research (CIO), University of Groningen, Groningen, The Netherlands

(12) Cooperative Institute for Research in Environmental Sciences (CIRES), University of Colorado, Boulder, CO, USA

Correspondence to: Z. Wang (zhiting@iup.physik.uni-bremen.de)

25

Abstract

Inverse modeling is a useful tool to retrieve CH₄ fluxes; however, evaluation of the applied chemical transport model is an important step before using the inverted emissions. For inversions using column data one concern is how well the model represents stratospheric and tropospheric CH₄ respectively

30 when assimilating total column measurements. In this study atmospheric CH₄ from three inverse
models is compared to FTS (Fourier Transform Spectrometry), satellite and in situ measurements.
Using the FTS measurements the model biases are separated into stratospheric and tropospheric
contributions. When averaged over all FTS sites the model bias amplitudes (absolute model to FTS
differences) are 7.4±5.1 ppb, 6.7±4.8 ppb, and 8.1±5.5 ppb in the troposphere for the models TM3,
35 TM5-4DVAR, LMDz-PYVAR, respectively, and 4.3±9.9 ppb, 4.7±9.9 ppb, and 6.2±11.2 ppb in the
stratosphere. The tropospheric model biases show a latitudinal gradient for all models, however there
are no clear latitudinal dependencies for stratospheric model biases visible except with the LMDz-
PYVAR model. The latitudinal gradient is not present in a comparison with in situ measurements,
which is attributed to the different longitudinal coverage of FTS and in situ measurements. Similarly, a
40 latitudinal pattern exists in model biases in vertical CH₄ gradients in the troposphere, which indicates
vertical transport of tropospheric CH₄ is not represented correctly in the models.

1 Introduction

Atmospheric methane (CH₄) is the second most important anthropogenic greenhouse gas. Atmospheric
CH₄ concentrations began to rise again in 2007 after a decade of near-zero growth (Rigby et al., 2008).
45 Possible explanations for the stability of CH₄ concentrations during 1999-2006 include: an increase in
anthropogenic emissions and coincident decrease in wetland emissions (Bousquet et al., 2006);
decreased northern hemisphere microbial sources (Kai et al., 2011); and a combination of decreasing-
to- stable fossil fuel emissions and stable-to-increasing microbial emissions (Kirschke et al., 2013).
Several possible reasons for the renewed growth of CH₄ concentrations after 2006 have been proposed
50 including the increase of wetland emissions during 2007 and 2008 in either the tropics, owing to greater
than average precipitation, and/or in the Arctic, owing to high temperatures (Dlugokencky et al., 2009),
the anthropogenic contribution in the tropics and mid-latitudes in the northern hemisphere during the
period 2007-2010 (Bergamaschi et al., 2013), an increase of emissions from oil- and gas production and
use during 2007-2014 (Hausmann et al., 2016), and from agriculture (Schaefer et al., 2016).
55 Prediction of the evolution of CH₄ in the atmosphere requires knowledge of the sources and sinks.
Inverse modeling is usually used to retrieve fluxes from observations of atmospheric concentrations.
The commonly used measurements include surface measurements from global networks, such as the
NOAA/ESRL (Earth System Research Laboratory of the National Oceanic and Atmospheric
Administration), and total column data from satellites, such as the SCIAMACHY (Scanning Imaging
60 Absorption Spectrometer for Atmospheric Chartography) or GOSAT (Greenhouse gases Observing
SATellite). However, compared to total column data the surface measurements characterize the
boundary layer only and CH₄ concentrations in the boundary layer are sensitive to boundary layer
height that is difficult to be accurately simulated in a global transport model. The total column
measurements are less sensitive to model errors in the vertical distributions of CH₄, however, they are
65 also only sensitive to broader-scale signatures. Compared to satellite measurements surface in-situ
measurements have poor spatial coverage but are more precise and less subject to biases. Total column
measurements of CH₄ include a contribution from the stratosphere where the concentrations are

influenced by dynamical processes like meridional transport, tropopause variations, and subsidence associated with the polar vortex, and chemistry. If a transport model does not accurately simulate these processes, the retrieved sources and sinks using total column measurements will not be correct (Locatelli et al., 2015a; 2015b). Especially in the polar region, the tropopause height varies strongly and the dynamical processes are complex. Turner et al. (2015) compared GOSAT CH₄ with GEOS-Chem simulations, and found large differences at high-latitudes. They proposed that the model bias in total column CH₄ at high- latitudes comes from the stratosphere since the validation with TCCON (Total Carbon Column Observing Network), NOAA surface and aircraft measurements, and HIPPO shows good performances of the model in the troposphere. Ostler et al. (2016) assessed accuracies of models in the stratosphere by replacing modeled stratospheric CH₄ with satellite measurements. They found that modeled stratospheric CH₄ shows large scatter and the corrected total columns of CH₄ show improved or degraded agreements with TCCON measurements depending on the used satellites and models. These results imply that satellite-based stratospheric CH₄ is not accurate enough to resolve a possible stratospheric contribution to model biases in total column CH₄ as uncovered by TCCON. TCCON-based measurements could fulfill such a role, as presented in Saad et al. (2016) and this study. Using HF as a proxy, Saad et al. (2016) derived tropospheric CH₄ products and investigated the impact of stratospheric and tropospheric model biases in GEOS-Chem on inversions. They found an increasing stratospheric mismatch with decreasing tropopause altitudes and a phase lag in modeled tropospheric seasonality. A small bias in the modeled CH₄ column could come from counteracting stratospheric and tropospheric model errors. They noted that the tropospheric time lag can produce large errors in posterior wetland emissions in high northern latitudes.

In this study the model biases in the stratosphere and troposphere are assessed with respect to the latitudinal pattern. In order to investigate the accuracy of the models several measurements are used: (i) total, tropospheric and stratospheric column-averaged CH₄ mole fractions measured at the TCCON (Wunch et al., 2011; Wang et al., 2014), which are used to separate stratospheric and tropospheric contributions to model bias in total columns, (ii) total column-averaged CH₄ mole fraction measured by GOSAT (Parker et al., 2011) and CH₄ profiles measured by TES (Tropospheric Emission Spectrometer) (Worden et al., 2012), (iii) surface CH₄ measured within the NOAA network (Dlugokencky et al., 1994) and (iv) in situ CH₄ profiles from aircraft campaign HIPPO (HIAPER Pole-to-Pole Observations) (Wofsy et al., 2012). In the following, Sect. 2 presents the measurements, models and analysis approach, while Sect. 3 presents the results and discussions. Conclusions are drawn in Sect. 4.

2 Measurements and models

We work here with near-infrared spectra of TCCON, from which the tropospheric CH₄ is derived using an a posteriori correction method in contrast to the direct profile retrieval (Sepulveda et al., 2014) being applied to mid-infrared spectra. The tropospheric CH₄ is derived through removing stratospheric contributions in total column CH₄. The stratospheric contributions are estimated from stratospheric N₂O columns derived from total N₂O columns. A calibration of the method against in-situ measurements shows an agreement within 3.0±2.0 ppb (see Figure 1). Given the total and tropospheric CH₄ columns,

stratospheric column-averaged CH₄ is derived using knowledge of the tropopause pressure. The TCCON sites used in this study are listed in Table 1, the products are all using the GGG2014 version (Wunch et al., 2015), except for at Ny-Ålesund.

110 The CO₂ proxy retrieval method (Frankenberg et al., 2011) is applied in GOSAT data, which infers dry
air columns from the CO₂ columns retrieved from the same spectra as used in the CH₄ retrieval. This
method assumes the CO₂ concentrations are known and provided by model simulations (the
CarbonTracker model). The GOSAT total column-averaged dry-air CH₄ mole fractions used here are
version UoL-OCPRv7 and only spectra measured in clear sky conditions are used (Parker et al., 2011).
115 GOSAT has a ground footprint diameter of about 10.5 km and 4 seconds exposure duration. The TES
instrument measures atmospheric radiances from which atmospheric profiles are inferred using an
optimal estimation algorithm subject to a priori constraints. The CH₄ retrieval of TES has a DOFS
(degree of freedom for signal) about 0.8~2.3, which peaks in the tropics and decrease toward high
latitudes. The version F07_10 data are applied and measurements with less than 1.4 DOFS are filtered
out. Validation of F07_10 data against to HIPPO measurements shows a bias of -8~5 ppb with standard
120 deviations of 25~50 ppb below 100 hPa (Herman and Osterman, 2014).

Vertical gradients of tropospheric CH₄ can be qualitatively calculated by using the comparative
tropospheric column-averaged CH₄ and surface CH₄. Only long-term time scales are used here, and
variations with scales longer than 1.4 years are extracted from the time series of tropospheric and
surface CH₄. TCCON and in situ sites are selected to be located close to one another so that both
125 instruments measure similar airmasses. The sites and measurements are listed in Table 3.

The CH₄ measurements during HIPPO-1 to 5 are those made by a quantum cascade laser spectrometer
(QCLS). Calibrations derived through comparisons with NOAA Programmable Flask Package
measurements are applied.

130 The models used in this study are TM3, TM5-4DVAR, LMDz-PYVAR, whose details are given in
Table 3. All the three models are optimized against in situ measurements at the surface through
inversions of CH₄ surface emissions. The first two models used a common emission a priori for their
inversion runs. Detailed information on the inversion methodology is discussed in Bergamaschi et al.
(2015). The LMDz-PYVAR uses a different a priori and background stations as constraints, the BG-SP
135 setup described in Locatelli et al. (2015b). The chemical reactions considered in the models are the
oxidation by OH in the troposphere, and by Cl, OH and O(¹D) in the stratosphere. The fields of the
radicals are prescribed monthly with no interannual changes.

Details about the global atmospheric tracer model TM3 can be found in Heimann and Körner (2003)
and the inversion method of the Jena CarboScope is described in Rödenbeck (2005). TM5-4DVAR is a
four-dimensional data assimilation system for inverse modeling of atmospheric methane emission
140 (Meirink et al., 2008). The system is based on the TM5 atmosphere transport model (Krol et al., 2005).
LMDz-PYVAR is a framework that combines the inversion system PYVAR (Chevallier et al., 2005;
Pison et al., 2009) with the transport model LMDz (Hourdin et al., 2006).

For evaluation of the models, we interpolate the simulations in time, latitudes, longitudes and pressure to match the measurements. For the total and tropospheric column-averaged CH₄ the model profile is integrated taking the a priori and averaging kernel into account according to Rodgers and Connor (2003) using Eq. 9 and 14 from Wang et al. (2014). In contrast to FTS and GOSAT the transformation of model CH₄ profiles to the counterpart of TES is done in logarithms of a priori and model quantities. The thermal tropopause calculated using the reanalysis data ERA-Interim is used in all calculations, which could not be so accurate for the TM5 and LMDz models, especially for LMDz that predicts its own meteorology fields through nudging to reanalysis data.

3 Comparison between measurements and models

The CH₄ column meridional distribution is sensitive to the latitudinal distribution of CH₄ sources and sinks, tropopause altitudes, inter-hemisphere transport in the troposphere, and the residual circulation in the stratosphere. Assessing latitudinal variabilities of biases of a model could reveal how well these processes are represented in the model. Another important concern of this study is to determine which of tropospheric or stratospheric model biases contributes more to the total bias. The model to FTS comparison covers the period 2007-2011 when FTS measurements are available and the comparison to GOSAT is for the period 2009-2011.

The latitudinal behavior of the model bias in total column-averaged CH₄ mole fractions is revealed by comparisons to FTS and GOSAT measurements as presented in Figure 2, similar to previous work (Monteil et al., 2013). CH₄ is emitted mainly in the northern hemisphere, destroyed mainly in the tropics by OH and has a slow inter-hemisphere transport with a temporal scale of approximately 1 year. CH₄ is transported into the stratosphere mostly in the tropics and back to the troposphere in the extratropics by the residual circulation. In the troposphere, CH₄ concentrations are higher in the northern hemisphere than in the southern hemisphere with a gradient throughout the tropics. In the stratosphere, CH₄ has a more or less symmetrical distribution between the two hemispheres. In Fig. 2 the model biases present a clear latitudinal dependence, similar to results revealed by other studies (e.g. Turner et al., 2015 and Alexe et al., 2015). The latitudinal dependence is similar between FTS and GOSAT northward of 50°S where FTS measurements are available. The model to measurements difference shows a North-South gradient with positive values at northern high-latitude northward of 50°S for all the models.

With FTS-derived tropospheric and stratospheric column-averaged CH₄ (Wang et al., 2014) it is possible to examine how the tropospheric and stratospheric columns contribute to the model bias in the total column-averaged CH₄ Figure 3 shows yearly and seasonal median model biases scaled by the fraction of the air column in the troposphere and stratosphere. It is clear that model biases in the troposphere exhibit a North-South gradient with positive values in northern high-latitude during all seasons for all models. In the stratosphere model biases do not present any clear latitudinal pattern that persists through the whole year, and show significant seasonal variabilities for TM3 and TM5-4DVAR. That is consistent with the fact that stratospheric CH₄ distributions cycle between summer and winter

180 hemispheric states. In the case of LMDz-PYVAR there is a permanent pattern in the stratospheric biases that is more negative in the south. This pattern is consistent with the North-South gradient in the total column biases. Comparing to Fig. 2 one can see that the latitudinal pattern of model biases in total column-averaged CH₄ results from both the stratosphere and troposphere for LMDz-PYVAR, but arises from the troposphere for TM3 and TM5. The model biases change signs yearly and seasonally, 185 therefore it is more appropriate to use the amplitudes (absolute model to FTS differences) to evaluate the contributions of the troposphere and stratosphere. The medians of model bias amplitudes over all FTS sites and years are 7.4±5.1 ppb in the troposphere and 4.3±9.9 ppb in the stratosphere for TM3, 6.7±4.8 ppb and 4.7±9.9 ppb for TM5-4DVAR, and 8.1±5.5 ppb and 6.2±11.2 ppb for LMDz-PYVAR.

190 Evaluations of the models at the surface using in-situ measurements, which are assimilated into the models, show smaller biases than the tropospheric column-averaged CH₄. The amplitudes are mostly below 10 ppb in the northern hemisphere except for a few outliers and below 5 ppb in the southern hemisphere (not shown). The model biases at the surface do not show any significant latitudinal dependence. It is not clear how the model biases at the surface appear in the regions where no measurements are assimilated. However, it could be true that the overestimation of the tropospheric 195 CH₄ meridional gradient is due to model biases in the mid and upper troposphere. That would mean that vertical distributions of CH₄ in the troposphere are not represented correctly in the models.

Figure 4 presents a comparison of modeled and measured vertical gradients of tropospheric CH₄, as qualitatively represented by the difference between the tropospheric column-averaged CH₄ and the surface CH₄. The vertical gradient is influenced by surface emissions, transport and OH fields. 200 Generally there are negative vertical gradients in the northern hemisphere and positive vertical gradients in the southern hemisphere (except for over the southern continents in locations with strong emissions). Here we refer to decreasing CH₄ mole fractions with altitude as a negative vertical gradient, while increasing CH₄ with altitude is a positive vertical gradient. This occurs because most CH₄ is emitted in the northern hemisphere and mixed into the southern hemispheric Hadley cell, whose southward branch prevails in the mid and upper troposphere. In the troposphere, surface emissions cause decreasing CH₄ with altitude, while OH oxidation causes a negative vertical gradient. The model 205 biases in the tropospheric vertical gradient are mostly positive in mid and high northern latitudes, and negative at other latitudes. So the overestimated tropospheric CH₄ in mid and high northern latitudes could not originate from overestimated emissions, which should result in a more negative vertical gradient in the troposphere. 210

Figure 5 shows a comparison between model simulations and HIPPO measurements. The results are longitudinally averaged for all five HIPPO missions within grids of 4° latitude and pressure increments of 10 hPa. A significant feature is an overestimation of CH₄ in the lowermost stratosphere over latitudes higher than 30°S/N, much larger than the biases in the troposphere. It is not clear whether the 215 overestimation arises from the residual transport in the stratosphere, which appears to be too strong, a too high tropopause, an incorrect vertical CH₄ gradient across the tropopause or misrepresentation of stratospheric chemistry. Underestimations dominate in the upper southern troposphere, consistent with the results in Fig. 4 that modeled gradients of tropospheric CH₄ are biased negative as revealed by FTS

220 and surface measurements. There are no significant patterns for the vertical gradient bias in the northern troposphere.

Unlike for the FTS, the model biases in the tropospheric column-averaged CH₄ revealed by HIPPO do not show a significant latitudinal trend (Fig. 6, only TM3 are shown there since other models gives similar behavior). This could be because the FTS measured tropospheric CH₄ is defined differently than the mean mole fraction between the surface and thermal tropopause. In deriving the FTS tropospheric CH₄, the stratospheric CH₄ is removed via its linear correlation with N₂O. The tropopause in the FTS data therefore has a chemical definition. It is not clear how different from each other the two kinds of tropopause are during this period. A sensitivity test was conducted by shifting the thermal tropopause 200 hPa upward to include the lower stratosphere where CH₄ is overestimated by the models. The model biases compared against HIPPO then become closer to those against FTS. However, this difference of 200 hPa between the chemical and thermal tropopause is unrealistically large. In addition, the FTS measured tropospheric CH₄ agrees well with in situ measurements in Fig. 1 where the thermal tropopause is applied.

Another possible explanation is that HIPPO sampled the atmosphere mostly in the region 150°E~110°W, over the Pacific Ocean. Apart from Izaña and Ny-Ålesund, the northern FTS sites are located inland. The longitudinal dependence of model biases is investigated with TES measured CH₄ mole fractions at 215, 464 and 680 hPa (the lower panel in Fig. 6). Because the TES profiles have limited vertical resolution, the concentrations at the three levels are not independent. The weighting function of CH₄ at 215 hPa peaks around 200 hPa in the tropics and around the 300 hPa higher than 50°N/S. The measurements at 464 hPa show the largest sensitivity around 500~600 hPa, and those at 680 hPa have similar vertical sensitivity but less weights above 400 hPa. The comparisons are separated into a region representing HIPPO sampling (referred as region I) and the remaining longitudes (referred as region II). Differences between the model biases in the two regions occur northward of 45°N most significantly at the level 215 hPa. Increases in the model biases continue in region II but decrease in region I, which is more or less similar to the differences between model biases revealed by FTS and HIPPO in these latitudes. Consistent with FTS the model-TES difference also shows a North-South gradient northward of 50°S. However, it is not clear whether the latitudinal pattern comes from the TES retrieval or model errors. Validation of TES tropospheric CH₄ with HIPPO gives near zeros biases except for latitudes 40°~60°N where the TES biases vary in -10~-20 ppb (Herman and Osterman, 2014).

250 **4 Conclusions**

In this study, three inverse models for CH₄ are evaluated using different observations that cover different scales. The aim is to determine whether most of the model biases are located in the stratosphere or troposphere. With FTS stratospheric and tropospheric column-averaged CH₄, retrieved from total column FTS measurements, it is shown that model bias amplitudes are 7.4±5.1 ppb, 6.7±4.8 ppb, and 8.1±5.4 ppb in the troposphere for TM3, TM5-4DVAR, and LMDz39-PYVAR. The

corresponding stratospheric biases are 4.3 ± 9.9 ppb, 4.7 ± 9.9 ppb, and 6.1 ± 11.2 ppb, respectively. The tropospheric model bias exhibits a North-South gradient northward of 50°S with an overestimation in northern high-latitude for all models. There is no persistent latitudinal pattern with season in the stratospheric model bias for TM3 and TM5-4DVAR.

260 The evaluation of the models at the surface shows a smaller bias compared to the tropospheric column-
averaged CH_4 . We assume that the tropospheric model biases are mainly located in the middle and
upper troposphere although comparisons at the surface are only limited to sites where the measurements
have been assimilated into the models. Comparison with HIPPO in the troposphere does not show the
same latitudinal pattern in model biases as in the comparison with FTS. Two possible reasons are
265 suggested: (i) the difference between the thermal tropopause and that in the FTS tropospheric CH_4
product, (ii) the latitude patterns of model biases are dependent on longitude. Using an assessment of
model biases relative to TES satellite measurements, we propose that the longitudinal dependence of
the model performance contributes to the difference between HIPPO and FTS. However, the tropopause
altitude could cause differences during short temporal scale processes, e.g. stratospheric intrusions
270 where the stratospheric air can sink below the thermal tropopause. Stratospheric air can also detach
from the stratosphere completely and enter the troposphere. If the detached air parcels still have
stratospheric properties, e.g. CH_4 correlates with N_2O as in the stratosphere, the FTS measured
tropospheric CH_4 would exclude these air parcels; however, direct integration from the surface to the
thermal tropopause, such as that used for the models and in situ profiles will include these in the
275 tropospheric CH_4 . More confusing situations could occur where there is strong mixing across the UTLS
(the upper troposphere and lower stratosphere) and both thermal and chemical tropopause are not well
defined. Future works will be devoted to clarifying the realistic content in FTS tropospheric CH_4 and to
defining a reasonable approach to comparing it with in situ and model products in these situations.

Acknowledgements

280 This research is funded by EU project InGOS. We acknowledge funding from the European Union's
Horizon 2020 research and innovation program for the project RINGO (grant agreement No 730944) as
well. TCCON data were obtained from the TCCON Data Archive, hosted by the Carbon Dioxide
Information Analysis Center (CDIAC) - tcon.onrl.gov. The TM5-4DVAR data is from Peter
Bergamaschi at European Commission Joint Research Centre, Institute for Environment and
285 Sustainability, Italy. Lamont-AirCore measurements have been provided by the Colm Sweeney at the
NOAA Carbon Cycle and Greenhouse Gas Group Aircraft Program
(<http://www.esrl.noaa.gov/gmd/ccgg/aircraft/>). Nicholas Deutscher is supported by an ARC- DECRA
Fellowship, DE140100178. TCCON measurements at Park Falls and Lamont are possible thanks to
NASA grants NNX14AI60G, NNX11AG01G, NAG5-12247, and NNG05-GD07G, and the NASA
290 Orbiting Carbon Observatory Program, as well as technical support from the DOE ARM program
(Lamont) and Jeff Ayers (Park Falls). Darwin and Wollongong TCCON support is funded by NASA
grants NAG5-12247 and NNG05-GD07G and the Australian Research Council grants DP140101552,
DP110103118, DP0879468 and LP0562346, as well as support from the GOSAT project and DOE

ARM technical support in Darwin. The EU projects InGOS and ICOS-INWIRE and the Senate of Bremen provide financial support for TCCON measurements at Bremen, Orleans, Bialystok and Ny Alesund, and Orleans is also supported by the RAMCES team at LSCE. The Lauder TCCON programme is core-funded by NIWA through New Zealand's Ministry of Business, Innovation and Employment.

References

- Alexe, M., Bergamaschi, P., Segers, A., Detmers, R., Butz, A., Hasekamp, O., Guerlet, S., Parker, R., Boesch, H., Frankenberg, C., Scheepmaker, R. A., Dlugokencky, E., Sweeney, C., Wofsy, S. C., and Kort, E. A.: Inverse modeling of CH₄ emissions for 2010–2011 using different satellite retrieval products from GOSAT and SCIAMACHY, *Atmos. Chem. Phys.*, 15, 113–133, doi:10.5194/acp-15-113-2015, 2015.
- Bousquet, P., Ciais, P., Miller, J. B., Dlugokencky, E. J., Hauglustaine, D. A., Prigent, C., Van der Werf, G. R., Peylin, P., Brunke, E. G., Carouge, C., Langenfelds, R. L., Lathiere, J., Papa, F., Ramonet, M., Schmidt, M., Steele, L. P., Tyler, S. C., and White, J.: Contribution of anthropogenic and natural sources to atmospheric methane variability, *Nature*, 443, 439–443, 2006.
- Bergamaschi, P., Houweling, S., Segers, A., Krol, M., Frankenberg, C., Scheepmaker, R. A., Dlugokencky, E., Wofsy, S. C., Kort, E. A., Sweeney, C., Schuck, T., Brenninkmeijer, C., Chen, H., Beck, V., Gerbig, C.: Atmospheric CH₄ in the first decade of the 21st century: Inverse modeling analysis using SCIAMACHY satellite retrievals and NOAA surface measurements, *J. Geophys. Res.*, 118, 7350–7369. doi:10.1002/jgrd.50480, 2013.
- Bergamaschi, P., Corazza, M., Karstens, U., Athanassiadou, M., Thompson, R. L., Pison, I., Manning, A. J., Bousquet, P., Segers, A., Vermeulen, A. T., Janssens-Maenhout, G., Schmidt, M., Ramonet, M., Meinhardt, F., Aalto, T., Haszpra, L., Moncrieff, J., Popa, M. E., Lowry, D., Steinbacher, M., Jordan, A., O'Doherty, S., Piacentino, S., and Dlugokencky, E.: Top-down estimates of European CH₄ and N₂O emissions based on four different inverse models, *Atmos. Chem. Phys.*, 15, 715–736, doi:10.5194/acp-15-715-2015, 2015.
- Blumenstock, T., Hase, F., Schneider, M., García, O. E., Sepúlveda, E.: TCCON data from Izana, Tenerife, Spain, Release GGG2014R0. TCCON data archive, hosted by the Carbon Dioxide Information Analysis Center, Oak Ridge National Laboratory, Oak Ridge, Tennessee, USA. <http://dx.doi.org/10.14291/tccon.ggg2014.izana01.R0/1149295>, 2014.
- Chevallier, F., Fisher, P., Serrar, S., Bousquet, P., Breon, F.-M., Chedin, A., and Ciais, P.: Inferring CO sources and sinks from satellite observations: Method and application to TOVS data, *J. Geophys. Res.*, 110, D24309, doi:10.1029/2005JD, 2005.
- Dlugokencky, E. J., Steele, L. P., Lang, P. M., Masarie, K. A.: The growth rate and distribution of atmospheric methane, *J. Geophys. Res.*, 99, 17021–17043, 1994.
- Dlugokencky, E., Bruhwiler, L., White, J., Emmons, L., Novelli, P., Montzka, S., Masarie, K., Crotwell,

- 330 A., Miller, J., and Gatti, L.: Observational constraints on recent increases in the atmospheric CH₄ burden, *Geophys. Res. Lett.*, 36, L18803, doi:10.1029/2009GL039780, 2009.
- Deutscher, N. M., Griffith, D. W. T., Bryant, G. W., Wennberg, P. O., Toon, G. C., Washenfelder, R. A., Keppel-Aleks, G., Wunch, D., Yavin, Y., Allen, N. T., Blavier, J.-F., Jiménez, R., Daube, B. C., Bright, A. V., Matross, D. M., Wofsy, S. C., and Park, S.: Total column CO₂ measurements at Darwin, Australia – site description and calibration against in situ aircraft profiles, *Atmos. Meas. Tech.*, 3, 947-958, doi:10.5194/amt-3-947-2010, 2010.
- 335 Eskridge, R.E., Ku, J. Y., Rao, S.T., Porter, P. S., and Zurbenko, I. G.: Separating Different Scales of Motion in Time Series of Meteorological Variables, *Bull. Amer. Meteor. Soc.*, 78, 1473–1483, 1997.
- Frankenberg, C., Aben, I., Bergamaschi, P., Dlugokencky, E. J., Hees, R. V., Houweling, S., Meer, P. V. D., Snel, R. and Tol, P.: Global column-averaged methane mixing ratios from 2003 to 2009 as derived from SCIAMACHY: Trends and variability, *J. Geophys. Res.*, 116, D04302–D04302, 2011.
- 340 Geibel, M. C., Messerschmidt, J., Gerbig, C., Blumenstock, T., Chen, H., Hase, F., Kolle, O., Lavric, J. V., Notholt, J., Palm, M., Rettinger, M., Schmidt, M., Sussmann, R., Warneke, T., and Feist, D. G.: Calibration of column-averaged CH₄ over European TCCON FTS sites with airborne in-situ measurements, *Atmos. Chem. Phys.*, 12, 8763–8775, doi:10.5194/acp-12-8763-2012, 2012.
- 345 Hausmann, P., Sussmann, R., and Smale, D.: Contribution of oil and natural gas production to renewed increase in atmospheric methane (2007–2014): top–down estimate from ethane and methane column observations, *Atmos. Chem. Phys.*, 16, 3227-3244, doi:10.5194/acp-16-3227-2016, 2016.
- Heimann, M., and S. Körner, *The Global Atmospheric Tracer Model TM3: Model description and users manual release 3.8a*, Tech. Rep. 5, Max Planck Inst. for Biogeochem., Jena, Germany, 2003.
- 350 Hourdin, F., Musat, I., Bony, S., Braconnot, P., Codron, F., Dufresne, J. L., Fairhead, L., Filiberti, M. A., Friedlingstein, P., Grandpeix, J. Y., Krinner, G., Li, Z. X., and Lott, F.: The LMDz4 general circulation model: climate performance and sensitivity to parametrized physics with emphasis on tropical convection, *Climate Dynamics*, 27, 787-813, 2006.
- 355 Herman, R. and Osterman, G. (editors), Alvarado, M., Boxe, C., Bowman, K., Cady-Pereira, K., Clough, T., Eldering, A., Fisher, B., Fu, D., Herman R., Jacob, D., Jourdain, L., Kulawik, S., Lampel, M., Li, Q., Logan, J., Luo, M., Megretskaia, I., Nassar, R., Osterman, G., Paradise, S., Payne, V., Revercomb, H., Richards, N., Shephard, M., Tobin, D., Turquety, S., Vlnrotter, F., Wecht, K., Worden, H., Worden, J., Zhang, L., *Earth Observing System (EOS) Tropospheric Emission Spectrometer (TES) Data Validation Report (version F07_10 data)*, JPL Internal Report D-33192, 2014.
- 360 Hausmann, P., Sussmann, R., and Smale, D.: Contribution of oil and natural gas production to renewed increase in atmospheric methane (2007–2014): top–down estimate from ethane and methane column observations, *Atmos. Chem. Phys.*, 16, 3227-3244, doi:10.5194/acp-16-3227-2016, 2016.
- Kai, F. M., Tyler, S. C., Randerson, J. T., and Blake, D. R.: Reduced methane growth rate explained by decreased Northern Hemisphere microbial sources, *Nature*, 476, 194–197, 2011.

- 365 Krol, M., Houweling, S., Bregman, B., van den Broek, M., Segers, A., van Velthoven, P., Peters, W., Dentener, F., and Bergamaschi, P.: The two-way nested global chemistry-transport zoom model TM5: algorithm and applications, *Atmos. Chem. Phys.*, 5, 417-432, doi:10.5194/acp-5-417-2005, 2005.
- Kirschke, S., Bousquet, P., Ciais, P., Saunois, M., Canadell, J. G., Dlugokencky, E. J., Bergamaschi, P., Bergmann, D., Blake, D. R., Bruhwiler, L., Cameron-Smith, P., Castaldi, S., Chevallier, F., Feng, L.,
370 Fraser, A., Heimann, M., Hodson, E. L., Houweling, S., Josse, B., Fraser, P. J., Krummel, P. B., Lamarque, J.-F., Langenfelds, R. L., Quéré, C. L., Naik, V., O'doherty, S., Palmer, P. I., Pison, I., Plummer, D., Poulter, B., Prinn, R. G., Rigby, M., Ringeval, B., Santini, M., Schmidt, M., Shindell, D. T., Simpson, I. J., Spahni, R., Steele, L. P., Strode, S. A., Sudo, K., Szopa, S., Werf, G. R. V. D., Voulgarakis, A., Weele, M. V., Weiss, R. F., Williams, J. E. and Zeng, G.: Three decades of global methane sources and sinks, *Nature Geosci.*, 6(10), 813–823, doi:10.1038/ngeo1955, 2013.
- 375 Locatelli, R., Bousquet, P., Hourdin, F., Saunois, M., Cozic, A., Couvreux, F., Grandpeix, J.-Y., Lefebvre, M.-P., Rio, C., Bergamaschi, P., Chambers, S. D., Karstens, U., Kazan, V., van der Laan, S., Meijer, H. A. J., Moncrieff, J., Ramonet, M., Scheeren, H. A., Schlosser, C., Schmidt, M., Vermeulen, A., and Williams, A. G.: Atmospheric transport and chemistry of trace gases in LMDz5B: evaluation and implications for inverse modelling, *Geosci. Model Dev.*, 8, 129-150, doi:10.5194/gmd-8-129-2015, 2015a.
- 380 Locatelli, R., Bousquet, P., Saunois, M., Chevallier, F., and Cressot, C.: Sensitivity of the recent methane budget to LMDz sub-grid-scale physical parameterizations, *Atmos. Chem. Phys.*, 15, 9765-9780, doi:10.5194/acp-15-9765-2015, 2015b.
- 385 Meirink, J. F., Bergamaschi, P., and Krol, M. C.: Four-dimensional variational data assimilation for inverse modelling of atmospheric methane emissions: method and comparison with synthesis inversion, *Atmos. Chem. Phys.*, 8, 6341-6353, doi:10.5194/acp-8-6341-2008, 2008.
- Monteil, G., Houweling, S., Butz, A., Guerlet, S., Schepers, D., Hasekamp, O., Frankenberg, C., Scheepmaker, R., Aben, I., and Röckmann, T.: Comparison of CH₄ inversions based on 15 months of
390 GOSAT and SCIAMACHY observations, *J. Geophys. Res.*, 118, 11807–11823, doi:10.1002/2013JD019760, 2013.
- Messerschmidt, J., Macatangay, R., Notholt, J., Petri, C., Warneke, T. and Weinzierl, C.: Side by side measurements of CO₂ by ground-based Fourier transform spectrometry (FTS), *Tellus B*, 62(5), 749–758, doi:10.1111/j.1600-0889.2010.00491.x, 2010.
- 395 Messerschmidt, J., Chen, H., Deutscher, N. M., Gerbig, C., Grupe, P., Katrynski, K., Koch, F.-T., Lavrič, J. V., Notholt, J., Rödenbeck, C., Ruhe, W., Warneke, T., and Weinzierl, C.: Automated ground-based remote sensing measurements of greenhouse gases at the Białystok site in comparison with collocated in situ measurements and model data, *Atmos. Chem. Phys.*, 12, 6741-6755, doi:10.5194/acp-12-6741-2012, 2012.
- 400 Ostler, A., Sussmann, R., Patra, P. K., Houweling, S., De Bruine, M., Stiller, G. P., Haenel, F. J., Plieninger, J., Bousquet, P., Yin, Y., Saunois, M., Walker, K. A., Deutscher, N. M., Griffith, D. W. T.,

- Blumenstock, T., Hase, F., Warneke, T., Wang, Z., Kivi, R., and Robinson, J.: Evaluation of column-averaged methane in models and TCCON with a focus on the stratosphere, *Atmos. Meas. Tech.*, 9, 4843-4859, doi:10.5194/amt-9-4843-2016, 2016.
- 405 Parker, R., Boesch, H., Cogan, A., Fraser, A., Feng, L., Palmer, P. I., Messerschmidt, J., Deutscher, N., Griffith, D. W. T., Notholt, J., Wennberg, P. O. and Wunch, D.: Methane observations from the Greenhouse Gases Observing SATellite: Comparison to ground-based TCCON data and model calculations, *Geophys. Res. Lett. Geophysical Research Letters*, 38(15), doi:10.1029/2011gl047871, 2011.
- 410 Pison, I., Bousquet, P., Chevallier, F., Szopa, S., and Hauglustaine, D.: Multi-species inversion of CH₄, CO and H₂ emissions from surface measurements, *Atmos. Chem. Phys.*, 9, 5281-5297, doi:10.5194/acp-9-5281-2009, 2009.
- Rigby, M., Prinn, R. G., Fraser, P. J., Simmonds, P. G., Langenfelds, R. L., Huang, J., Cunnold, D. M., Steele, L. P., Krummel, P. B., Weiss, R. F., O'Doherty, S., Salameh, P. K., Wang, H. J., Harth, C. M., 415 Muhle, J., and Porter, L. W.: Re-newed growth of atmospheric methane, *Geophys. Res. Lett.*, 35, L22805, doi:10.1029/2008gl036037, 2008.
- Rödenbeck, C., Estimating CO₂ sources and sinks from atmospheric mixing ratio measurements using a global inversion of atmospheric transport, Technical Report 6, Max Planck Institute for Biogeochemistry, Jena, Germany, 2005.
- 420 Rodgers, C. D. and Connor, B. J.: Intercomparison of remote sounding instruments, *J. Geophys. Res.-Atmos.*, 108, 4116, doi:10.1029/2002JD002299, 2003.
- Sepúlveda, E., Schneider, M., Hase, F., Barthlott, S., Dubravica, D., García, O. E., Gomez-Pelaez, A., González, Y., Guerra, J. C., Gisi, M., Kohlhepp, R., Dohe, S., Blumenstock, T., Strong, K., Weaver, D., Palm, M., Sadeghi, A., Deutscher, N. M., Warneke, T., Notholt, J., Jones, N., Griffith, D. W. T., Smale, 425 D., Brailsford, G. W., Robinson, J., Meinhardt, F., Steinbacher, M., Aalto, T., and Worthy, D.: Tropospheric CH₄ signals as observed by NDACC FTIR at globally distributed sites and comparison to GAW surface in situ measurements, *Atmos. Meas. Tech.*, 7, 2337-2360, doi:10.5194/amt-7-2337-2014, 2014.
- Schaefer, H., Fletcher, S. E. M., Veidt, C., Lassey, K. R., Brailsford, G. W., Bromley, T. M., Dlugokencky, E. J., Michel, S. E., Miller, J. B., Levin, I., Lowe, D. C., Martin, R. J., Vaughn, B. H. and White, J. W. C.: A 21st-century shift from fossil-fuel to biogenic methane emissions indicated by ¹³CH₄, *Science*, 352(6281), 80–84, 2016.
- Schmidt, M., Lopez, M., Yver Kwok, C., Messenger, C., Ramonet, M., Wastine, B., Vuillemin, C., Truong, F., Gal, B., Parmentier, E., Cloué, O., and Ciais, P.: High-precision quasi-continuous 435 atmospheric greenhouse gas measurements at Trainou tower (Orléans forest, France), *Atmos. Meas. Tech.*, 7, 2283-2296, doi:10.5194/amt-7-2283-2014, 2014.
- Saad, K. M., Wunch, D., Deutscher, N. M., Griffith, D. W. T., Hase, F., De Mazière, M., Notholt, J.,

- 440 Pollard, D. F., Roehl, C. M., Schneider, M., Sussmann, R., Warneke, T., and Wennberg, P. O.: Seasonal variability of stratospheric methane: implications for constraining tropospheric methane budgets using total column observations, *Atmos. Chem. Phys.*, 16, 14003-14024, doi:10.5194/acp-16-14003-2016, 2016.
- Sherlock, V., Connor, B., Robinson, J., Shiona, H., Smale, D. and Pollard, D.: TCCON data from Lauder, New Zealand, 125HR, Release GGG2014R0, doi:10.14291/tccon.ggg2014.lauder02.R0/1149298, 2014.
- 445 Sussmann, R., Ostler, A., Forster, F., Rettinger, M., Deutscher, N. M., Griffith, D. W. T., Hannigan, J. W., Jones, N., and Patra, P. K.: First intercalibration of column-averaged methane from the Total Carbon Column Observing Network and the Network for the Detection of Atmospheric Composition Change, *Atmos. Meas. Tech.*, 6, 397-418, doi:10.5194/amt-6-397-2013, 2013.
- 450 Sussmann, R. and Rettinger, M.: TCCON data from Garmisch, Germany, Release GGG2014R0, TCCON data archive, hosted by the Carbon Dioxide Information Analysis Center, Oak Ridge National Laboratory, Oak Ridge, Tennessee, USA, doi:10.14291/tccon.ggg2014.garmisch01.R0/1149299, 2014.
- 455 Turner, A. J., Jacob, D. J., Wecht, K. J., Maasakkers, J. D., Lundgren, E., Andrews, A. E., Biraud, S. C., Boesch, H., Bowman, K. W., Deutscher, N. M., Dubey, M. K., Griffith, D. W. T., Hase, F., Kuze, A., Notholt, J., Ohyama, H., Parker, R., Payne, V. H., Sussmann, R., Sweeney, C., Velazco, V. A., Warneke, T., Wennberg, P. O., and Wunch, D.: Estimating global and North American methane emissions with high spatial resolution using GOSAT satellite data, *Atmos. Chem. Phys.*, 15, 7049-7069, doi:10.5194/acp-15-7049-2015, 2015.
- 460 Worden, J., Kulawik, S., Frankenberg, C., Payne, V., Bowman, K., Cady-Peirara, K., Wecht, K., Lee, J. E., and Noone, D.: Profiles of CH₄, HDO, H₂O, and N₂O with improved lower tropospheric vertical resolution from Aura TES radiances, *Atmos. Meas. Tech.*, 5, 397-411, doi:10.5194/amt-5-397-2012, 2012.
- 465 Wofsy, S. C., Daube, B. C., Jimenez, R., Kort, E., Pittman, J. V., Park, S., Commane, R., Xiang, B., Santoni, G., Jacob, D., Fisher, J., Pickett-Heaps, C., Wang, H., Wecht, K., Wang, Q.-Q., Stephens, B. B., Shertz, S., Watt, A. S., Romashkin, P., Campos, T., Haggerty, J., Cooper, W. A., Rogers, D., Beaton, S., Hendershot, R., Elkins, J. W., Fahey, D. W., Gao, R. S., Moore, F., Montzka, S. A., Schwarz, J. P., A. Perring, E., Hurst, D., Miller, B. R., Sweeney, C., Oltmans, S., Nance, D., Hints, E., Dutton, G., Watts, L. A., Spackman, J. R., Rosenlof, K. H., Ray, E. A., Hall, B., Zondlo, M. A., Diao, M., Keeling, R., Bent, J., Atlas, E. L., Lueb, R., Mahoney, M. J.: HIPPO Merged 10-second Meteorology, Atmospheric Chemistry, Aerosol Data (R_20121129). Carbon Dioxide Information Analysis Center, Oak Ridge National Laboratory, Oak Ridge, Tennessee, U.S.A. http://dx.doi.org/10.3334/CDIAC/hippo_010 (Release 20121129), 2012.
- 470 Wang, Z., Deutscher, N. M., Warneke, T., Notholt, J., Dils, B., Griffith, D. W. T., Schmidt, M., Ramonet, M., and Gerbig, C.: Retrieval of tropospheric column-averaged CH₄ mole fraction by solar absorption FTIR-spectrometry using N₂O as a proxy, *Atmos. Meas. Tech.*, 7, 3295-3305,

475 doi:10.5194/amt-7-3295-2014, 2014.

Wunch, D., Toon, G. C., Blavier, J.-F. L., Washenfelder, R., Notholt, J., Connor, B. J., Griffith, D. W. T., Sherlock, V., and Wennberg, P. O.: The Total Carbon Column Observing Network (TCCON), *Philos. Trans. R. Soc. A*, 369, 2087–2112, doi:10.1098/rsta.2010.0240, 2011.

480 Wunch, D., Toon, G. C., Sherlock, V., Deutscher, N. M., Liu, X., Feist, D. G., and Wennberg, P. O.: The Total Carbon Column Observing Network's GGG2014 Data Version. doi:10.14291/tccon.ggg2014.documentation.R0/1221662, 2015.

Wunch, D., Wennberg, P. O., Toon, G. C., Keppel-Aleks, G., Yavin, Y. G., Emissions of greenhouse gases from a North American megacity, *Geophys. Res. Lett.*, 36, L15810, 2009.

485 Washenfelder, R. A., Toon, G. C., Blavier, J.-F., Yang, Z., Allen, N. T., Wennberg, P. O., Vay, S. A., Matross, D. M. and Daube, B. C.: Carbon dioxide column abundances at the Wisconsin Tall Tower site, *Journal of Geophysical Research*, 111(D22), doi:10.1029/2006jd007154, 2006.

Table 1. Overview of TCCON sites used.

TCCON site	Latitude/°N	Longitude/°E	Altitude/masl	Citation
Ny-Ålesund	78.9	11.9	20	Messerschmidt et al., 2010
Sodankylä	67.3668	26.6310	188	
Bialystok	53.23	23.025	183	Messerschmidt et al., 2012
Bremen	53.10	8.85	27	Messerschmidt et al., 2010
Orléans	47.97	2.113	130	Messerschmidt et al., 2010
Garmisch	47.476	11.063	740	Sussmann et al., 2013, Sussmann and Rettinger, 2014
Park Falls	45.945	-90.273	440	Washenfelder et al., 2006
Lamont	36.604	-97.486	320	Wunch et al., 2009
Izaña	28.3	-16.483	2370	Blumenstock et al., 2014
Darwin	-12.424	130.891	30	Deutscher et al., 2010
Wollongong	-34.406	150.879	30	Deutscher et al., 2010
Lauder	-45.038	169.684	370	Sherlock et al., 2014

490

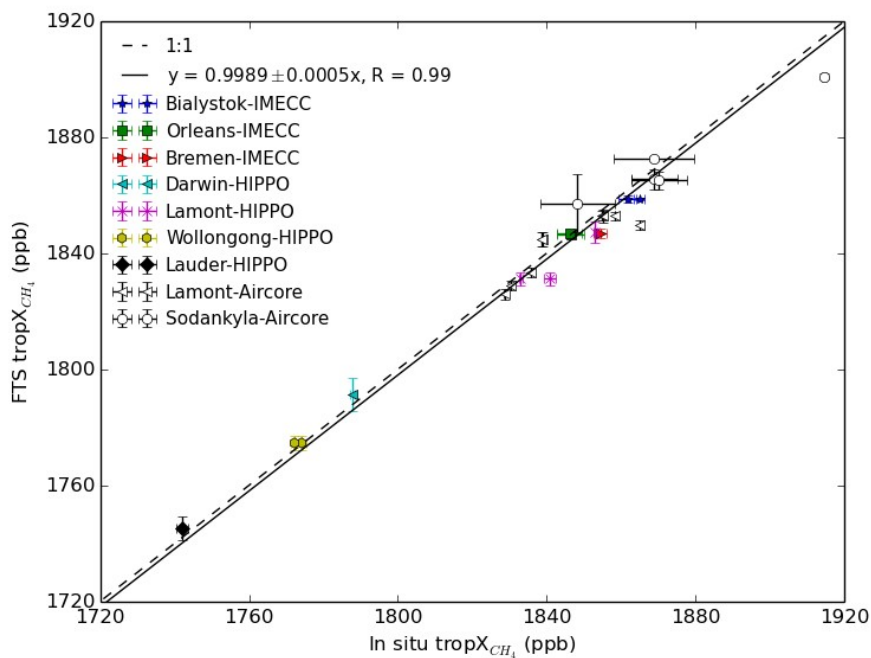
Table 2. Information on the models and setup details.

Model	Institute	Resolution (lat×lon)	No. of vertical levels	Output time step (hour)	Meteorology
TM3	Max Plank Institute for Biogeochemistry	4°×5°	26	3.0	ERA-Interim
TM5-4DVAR	European Joint Reseach Centre	1°×1° for Europe, 6°×4° for the rest of the world	25	1.5	ECMWF-IFS
LMDz-PYVAR	Laboratoire des Sciences du Climat et de l'Environnement	1.875°×3.75°	39	3.0	Prediction by LMDz with nudging to ECMWF reanalysis

Table 3. FTS and in-situ sites used for comparison to FTS tropospheric column-averaged CH₄ and surface/tower CH₄.

FTS site				In situ site			
Name	Lat/°N	Lon/°E	Alt/masl	Name	Lat/°N	Lon/°E	Alt/masl
Ny-Ålesund	78.923	11.923	24	Zep/NOAA	78.907	11.889	479
Sodankylä	67.367	26.631	188	Pal/NOAA	67.970	24.120	565
Orléans	47.965	2.113	132	Trainou tower	47.965	2.113	311
Park Falls	45.945	-90.273	440	Lef/NOAA	45.930	-90.270	868
Lamont	36.604	-97.486	320	Sgp/NOAA	36.620	-97.480	374
Izaña	28.300	-16.483	2370	Izo/NOAA	28.300	-16.480	2378
Lauder	-45.038	169.684	370	Bhd/NOAA	-41.408	174.871	90

500



505

Figure 1. Calibration results of FTS derived tropospheric column-averaged CH_4 mole fractions against in situ measurements. The in situ profiles are smoothed using GFIT CH_4 averaging kernels in the troposphere as described in Wang et al. (2014). The FTS data are averaged for the in situ measurement periods. The IMECC is an aircraft campaign over Europe (Geibel et al., 2012). The Lamont-AirCore measurements are from Greenhouse Gas Group Aircraft Program (<http://www.esrl.noaa.gov/gmd/ccgg/aircraft/>). The AirCore data at Sodankylä is from the FTS group there.

510

515

520

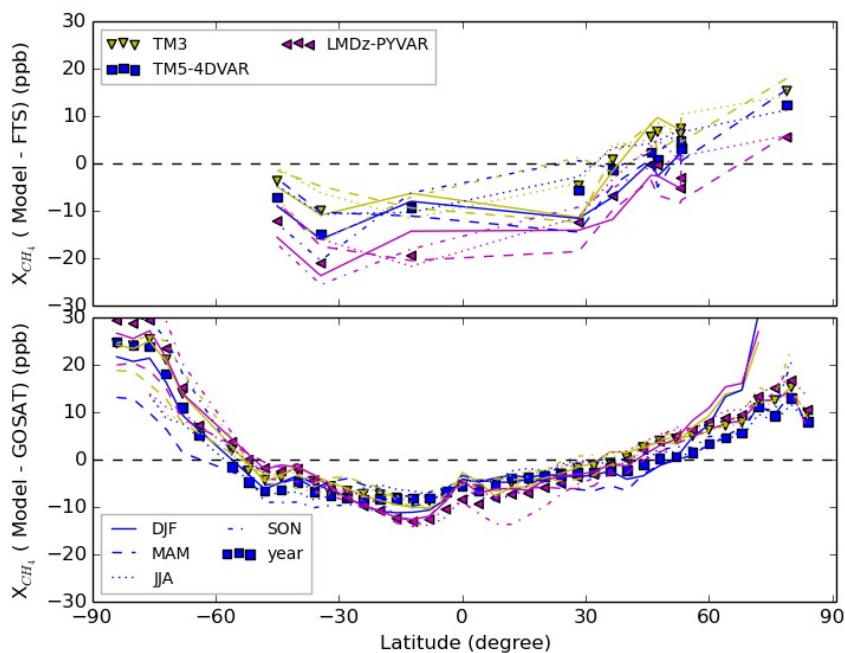
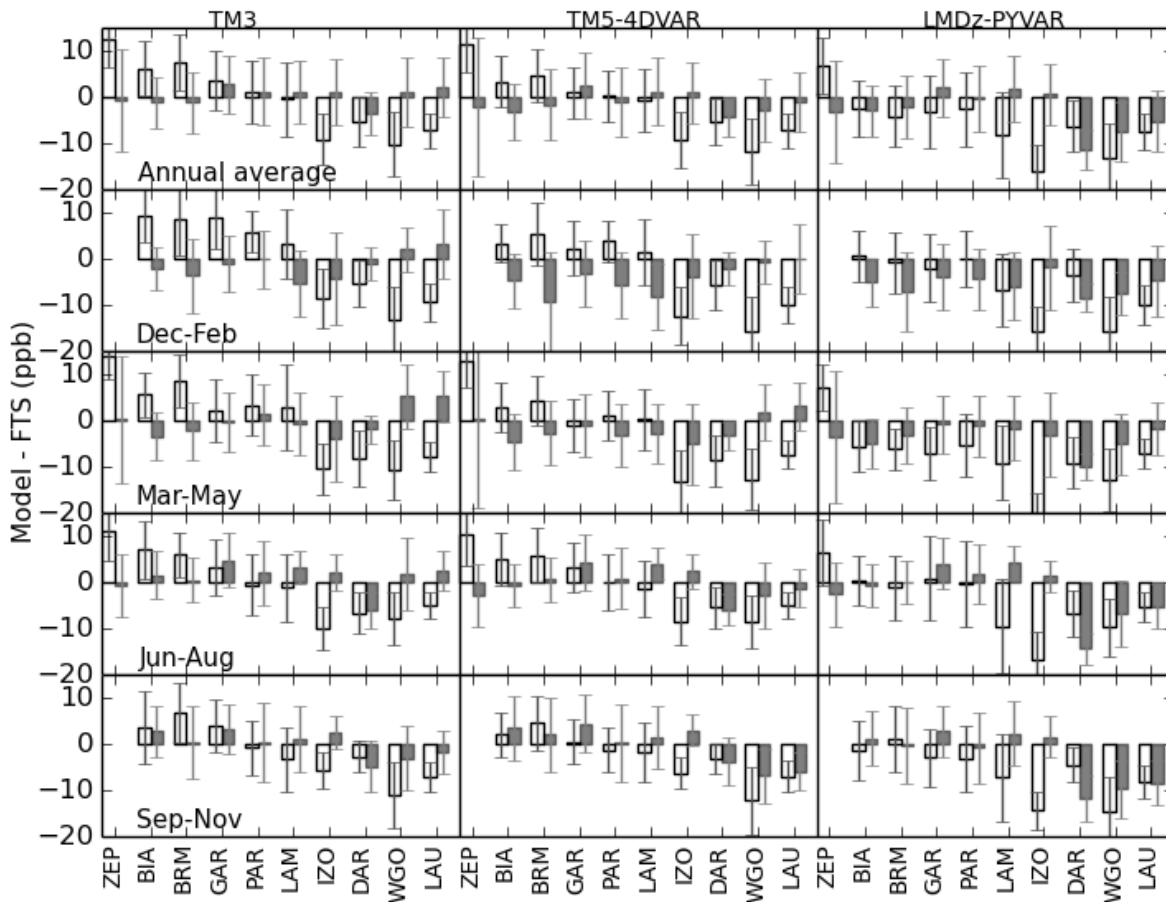


Figure 2. Yearly and seasonal mean model bias of total column-averaged CH_4 mole fractions plotted as a function of latitude. The upper panel is the results using FTS data while the lower panels is for GOSAT. The difference for the models is given in yellow (TM3), blue (TM5-4DVAR), and magenta (LMDz-PYVAR). The average of FTS results is for the period 2007-2011 where FTS measurements are available, and for GOSAT in the period 2009-2011.

530

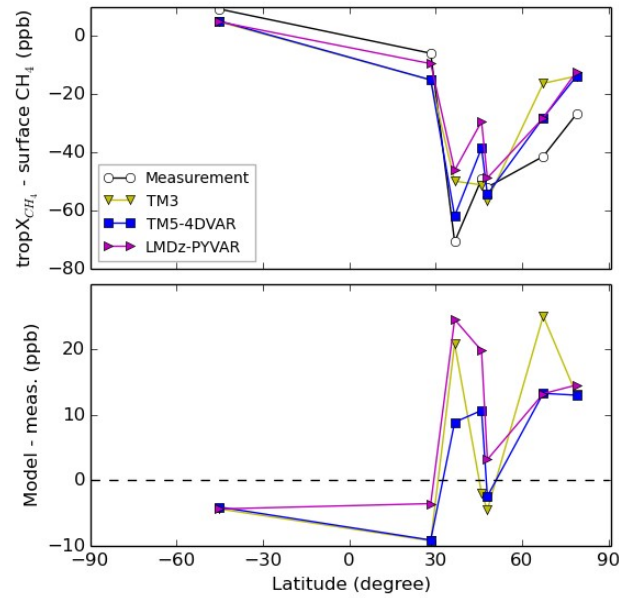


535

Figure 3. Yearly and seasonal medians of the scaled stratospheric and tropospheric contributions in modeled total column biases at TCCON sites. The sites from left to right is North to South. The white bar denotes the tropospheric bias, the grey bar for the stratospheric bias. The scale factor for the model bias are the air column fractions $P_t/1000$ (stratosphere) and $(1-P_t/1000)$ (troposphere), where P_t is the tropopause pressure. The error bar are the standard deviations of the model biases. The results are averaged for 2007-2011 when FTS measurements are available.

540

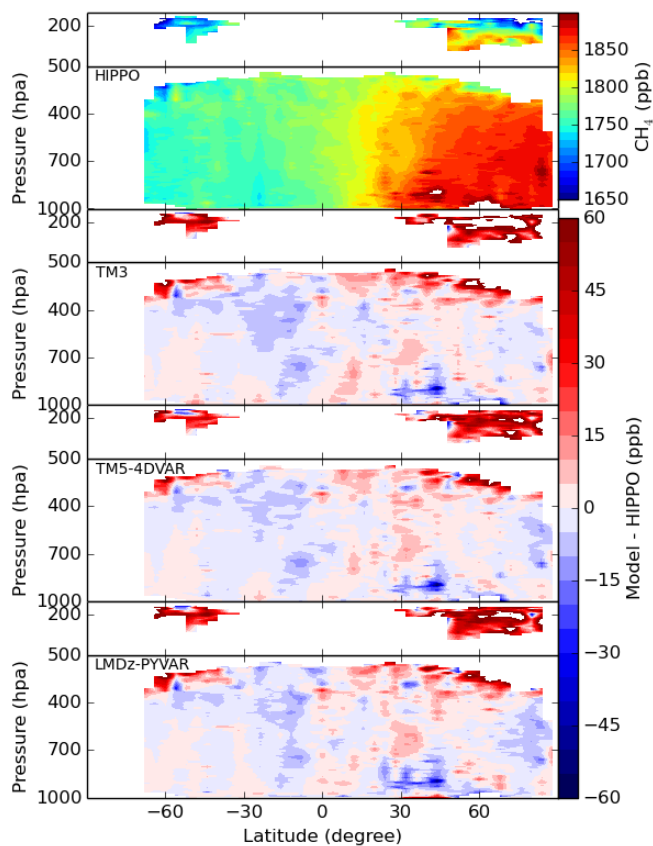
545



550 Figure 4. Measured (black) and simulated (yellow: TM3, blue: TM5-4DVAR, LMDz-PYVAR: magenta) vertical gradients of CH₄ in the troposphere (top panel) and differences between the measurement and simulations (lower panel) against latitude. The results are averaged for 2007-2011 when FTS measurements are available.

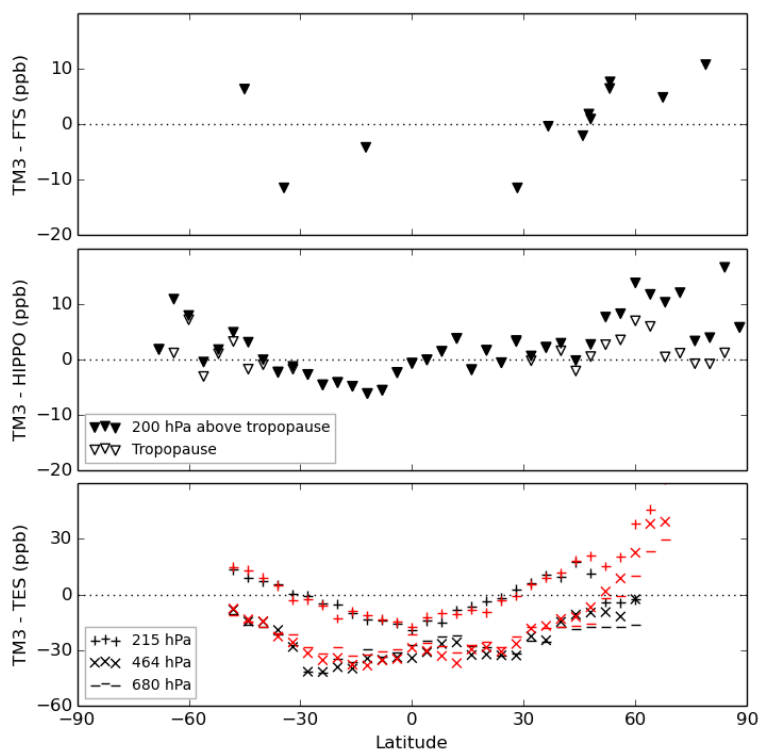
555

560



565 Figure 5. HIPPO measured CH_4 and differences with models in the stratosphere (short panel) and troposphere (high panel). The result is an average for five HIPPO missions, averaged for latitudinal bins of 4° and vertical increments of 10 hPa.

570



580 Figure 6. Comparisons of CH_4 between TM3 and (upper panel) FTS, (middle panel) HIPPO and (lower panel) TES. In the case of HIPPO and FTS tropospheric column-averaged CH_4 is compared, which is obtained from integration between surface and the tropopause (empty characters) or 200 hPa above the tropopause shifted (solid characters). For TES CH_4 mole fractions at 215 hPa, 464 hPa and 680 hPa are compared with TM3 simulations in a region $110^\circ\text{W}\sim 150^\circ\text{E}$ (black) and the region beyond it (red) separately. Both TM3 and measurements are averaged during HIPPO 1-5 period.